*Mdr*1 Transfection Causes Enhanced Apoptosis by Paclitaxel: An Effect Independent of Drug Efflux Function of P-Glycoprotein

Dong Li[1] and Jessie L.-S. Au[1,2,3]

Received February 26, 2001; accepted April 2, 2001

Purpose. We previously reported that in patient tumors the expression of the *mdr*1 p-glycoprotein (Pgp) resulted in a lower paclitaxel-induced inhibition of DNA precursor incorporation, but a higher apoptosis (*Clin. Cancer Res.* **4**:2949–2955, 1998). The present study was to evaluate these findings in an experimental system where the Pgp effect can be studied without confounding factors such as the intra- and inter-tumor heterogeneity associated with patient tumors.
Methods. To separate the effect of Pgp on intracellular paclitaxel accumulation from its effects on drug sensitivity, we compared the drug activity at various extracellular and intracellular drug concentrations using the human breast MCF7 tumor cells and its *mdr*1-transfected variant BC19 cells.
Results. Compared to MCF7 cells, BC19 cells showed a 9-fold higher Pgp level and >13-fold higher *mdr*1 expression. Intracellular paclitaxel accumulation was 80–130% lower in BC19 cells when the extracellular concentrations were ≤100 nM, but the difference was reduced to <15% differences at higher extracellular concentrations of ≥1,000 nM. For the G2/M block effect MCF7 cells were 43-fold more sensitive than BC19 cells at equal extracellular concentration, and 3.5-fold more sensitive at comparable intracellular concentrations. On the contrary, BC19 cells were more sensitive to the apoptotic effect; BC19 cells showed equal or higher apoptosis compared to MCF7 cells at extracellular concentrations above 100 nM, and a 30–100% higher apoptosis at comparable intracellular concentrations.
Conclusions. These results confirm our previous observations in patient tumors and indicate that enhanced Pgp expression is associated with enhanced sensitivity to the apoptotic effect of paclitaxel and reduced sensitivity to its G2/M block effect, via yet-unknown mechanisms that are unrelated to the effect of Pgp on intracellular drug accumulation.

KEY WORDS: paclitaxel; apoptosis; p-glycoprotein.

INTRODUCTION

Paclitaxel is one of the most important anticancer drugs developed in the past two decades. It has shown significant activity against human solid tumors, i.e. ovarian, head and neck, bladder, breast, and lung cancers (1). Paclitaxel enhances tubulin polymerization, promotes microtubule assembly and stabilizes microtubule dynamics, resulting in inhibition of cell proliferation and apoptosis (2–4). In human bladder, breast, head and neck, ovarian, and prostate tumors, paclitaxel inhibits tumor cell proliferation and induces apoptosis (5–9).

Studies using cell lines have indicated that increased drug efflux mediated by Pgp overexpression results in paclitaxel resistance (10). On the other hand, the significant activity of paclitaxel in doxorubicin-refractory breast cancer patients (11), which often exhibit Pgp overexpression (12), suggests that Pgp overexpression does not necessarily result in clinical resistance to paclitaxel. This is confirmed by the lack of correlation between Pgp status and prognosis in leukemia patients (13,14). To better understand the basis of these paradoxical observations, our laboratory has examined the relationship between paclitaxel-induced antiproliferation and apoptosis with tumor pathobiological properties including tumor stage, grade, labeling index (LI), and expression of Pgp, p53, and Bcl-2 in about 100 human bladder, breast, head and neck, ovarian, and prostate tumors (15). Our results indicate that the antiproliferative and apoptotic effects of paclitaxel are correlated with different tumor properties. The antiproliferative effect is inversely correlated with tumor stage, grade, LI and expression of Pgp, p53, and Bcl-2. The apoptotic effect is positively correlated with Pgp expression, LI and tumor grade, but is not related to tumor stage and expression of p53 and Bcl-2. We further found that the maximum sensitivity of individual tumors to the antiproliferative and apoptotic effects is inversely related, i.e. tumors that showed a lower maximum response to the antiproliferative effect displayed a higher maximum apoptosis. The different and often opposite relationships between the two effects and tumor pathobiological factors indicate that these effects are determined by different factors. Furthermore, because a drug effect is usually mediated by its intracellular concentration, the unparallel sensitivity of individual tumors to antiproliferation and apoptosis indicate that the two effects are determined by factors other than drug concentration. Finally, while the inverse relationship between Pgp expression and drug-induced antiproliferation may be due to the enhanced drug efflux in Pgp-positive tumors, the positive correlation between Pgp overexpression and drug-induced apoptosis is unexpected and suggests that biologic changes unrelated to drug efflux have resulted in enhanced apoptosis in the Pgp-positive tumors.

The two purposes of the present study were to evaluate the relationship between Pgp expression and the antiproliferative and apoptotic effects of paclitaxel in an experimental system where the Pgp effect can be studied without confounding factors such as the intra- and inter-tumor heterogeneity associated with patient tumors, and to test the hypothesis that the enhanced apoptosis and reduced G2/M block in Pgp-expressing cells is due to changes in tumor sensitivity to paclitaxel rather than, or in addition to, differential intracellular drug accumulation. The first goal was accomplished by comparing the concentration-response relationships in two cell lines which differ in their expression of Pgp, i.e. the human breast MCF7 carcinoma cells and the corresponding *mdr*1-transfected variant BC19 cells which over-express Pgp (16).

[1] College of Pharmacy, The Ohio State University, 500 West 12th Avenue, Columbus, Ohio 43210.
[2] Comprehensive Cancer Center, The Ohio State University, 500 West 12 th Avenue, Columbus, Ohio 43210.
[3] To whom correspondence should be addressed. (e-mail: Au.1@osu.edu)

ABBREVIATIONS: BSA, bovine serum albumin; FBS, fetal bovine serum; IC_{50}, concentration needed to produce 50% effect; LI, labeling index; PBS, phosphate-buffered saline; Pgp, p-glycoprotein; SRB, sulforhodamine; TBST, Tris buffered saline containing 0.1% Tween 20.

For the second goal which required a separation of the drug efflux effect of Pgp from other biologic consequences, first we established the extracellular drug concentrations that yielded equal intracellular drug concentrations in the two cell lines, and then we compared the drug effect at equal intracellular drug concentrations.

MATERIALS AND METHODS

Chemicals

Paclitaxel was a gift from the Bristol-Myers Squibb Co. (Wallingford, CT) and the National Cancer Institute (Bethesda, MD), and [^{3}H]paclitaxel (specific activity 19.3 μCi/mmol) from the National Cancer Institute. Cefotaxime sodium was purchased from Hoechst-Roussel (Somerville, NJ), gentamicin from Solo Pak Laboratories (Franklin Park, IL), other tissue culture supplies (i.e. RPMI 1640, L-glutamine, sodium pyruvate, fetal bovine serum (FBS)) from GIBCO Laboratories (Grand Island, NY), phenylmethylsulfonyl fluoride, sulforhodamine B (SRB) and propidium iodide from Sigma Chemical Co. (St. Louis, MO), mouse monoclonal antibody against Pgp (JSB-1) from BioGenex (San Ramon, CA), linked Streptoavidin-Biotin detection kit from Dako (Carpiteria, CA), and PCR primers from Genesys Inc. (Woodlands, TX). All chemicals and reagents were used as received.

Cell Culture Conditions

Human breast cancer cell lines, MCF7 and its *mdr*-1 transfected variant BC19 cells, were gifts from Dr. Kenneth Cowan (National Cancer Institute). The BC19 cells are stably transfected with *mdr*1 and do not require additional treatment to maintain the Pgp expression (16). The culture medium was RPMI 1640 medium supplemented with 10% FBS, 2 mM L-glutamine, 90 μg/ml gentamicin and 90 μg/ml cefotaxime sodium. Cells were incubated with complete medium at 37°C in a humidified atmosphere of 5% CO_2 in air. For experiments, cells were harvested from subconfluent cultures using trypsin and resuspended in fresh medium before plating. The cell cycle time, or the doubling time in exponentially growing cells, was 24 h for both cell lines.

Western Blot Analysis of Pgp

The procedures for Western blot analysis of Pgp were as described elsewhere (5). Briefly, cells were incubated in 10 mM KCl, 1.5 mM $MgCl_2$, 10 mM Tris-HCl (pH 7.4), 0.5% (w/v) SDS, and 1 mM phenylmethylsulfonyl fluoride for 10 min. The swollen cells were ruptured in a Dounce homogenizer (Pierce Chemical Co., Rockford, IL) with 20 or more strokes. After centrifugation at 15,000 × g for 20 min, the supernatant was analyzed for Pgp. Samples with equal amount of proteins were loaded on a 7.5% SDS-PAGE and transferred electrophoretically onto nitrocellulose membranes. Nitrocellulose membranes were blocked overnight in 5% skim milk in Tris-buffered saline containing 0.1% Tween 20 (TBST) and then washed twice with the same buffer. The membrane was incubated with antibody (1:500 dilution) for 1 h room temperature. The linker solution and peroxidase-conjugated streptavidin (1:5 dilution in TBST containing 1% BSA) were applied sequentially and then washed with TBST. The bands were developed using ECL Western blotting detection reagents (Amersham Life Science, Little Chalfont, Buckinghamshire, England).

Analysis of *mdr*1 Expression

The expression of *mdr*1 was determined using a semiquantitative RT-PCR method as described previously (17). This method is based on the relative amplification of a target gene and an endogenous gene (β-*actin*) which is used as an internal standard. The upstream primer for *mdr*1 was 5′-CCCATCATTGCAATAGCAGG-3′ and the downstream primer was 5′-GTTCAAACTTCTGCTCCTGA-3′, and the resulting fragment was 167 bp. The upstream primer for β-actin was 5′-GCGGGAAATCGTGCGTGACATT-3′ (BA-67), and the downstream primer was 5′-GATGGAGTT-GAAGGTTAGTTTCGTG-3′ (BA-68), and the resulting fragment was 328 bp.

Total cellular RNA was extracted using the acid guanidium thiocyanate-phenol-chloroform method (17). Cells were washed with PBS buffer and collected with denaturing solutions (4 M guanidine thiocyanate, 42 mM sodium citrate, 0.83% N-lauryl sarcosine, 0.2 mM β-mercaptoethanol). Cell suspension was mixed with 0.1 volume of 2 M sodium acetate, pH 4.0. After incubation on ice for 20 min, cells were extracted with phenol:chloroform:isoamyl alcohol (25:24:1). After centrifugation at 10,000 × g for 20 min at 4°C, RNA in the aqueous supernatant was transferred and precipitated with equal volume of isopropanol at –20°C for at least 30 min. The centrifugation and precipitation steps were repeated once. The resulting RNA pellet was washed with 75% ethanol, resuspended in 1 ml of RNase-free H_2O and stored at –20°C.

The amount of total RNA was quantitated by UV absorbance at 260 nm. RNA was reverse transcribed to cDNA as described previously (17). Briefly, 10 μg RNA were added to a master mixture containing 20 μl of 5× Reverse Transcriptase buffer, 5 μl of deoxyribonucleotide triphosphate (10 mM), 10 μl of dithiothreitol (10 mM), 2.5 μl of RNase (40,000 units/ml), 0.5 μl of random hexamers (0.45 units/ml), and 5 μl of MMTV reverse transcriptase (200 units/μl). Following incubation at 42°C for 1 h and 72°C for 10 min, the reaction was terminated by heating to 95°C for 3 min. The resulting cDNAs were stored at –20°C until analysis.

A series of cDNA dilutions were prepared and amplified in a reaction mixture consisting of 5 μl cDNA, 2.5 μl l0× PCR buffer, 0.5 μl deoxyribonucleotide triphosphate (10 mM), 1 μl of 3′ and 5′ primers (12.5 pmol/μl), 3.75 μl $MgCl_2$ (12.5 mM), 2 μl Taq DNA polymerase (500 units/ml), and 9.25 μl distilled H_2O. The reaction was carried out in a thermal cycler under the following conditions: 95°C for 5 min, 94°C for 40 s, 64°C for 60 s, and 72°C for 60 s. Following 29 cycles of PCR, a final extension at 72°C for 7 min was performed. Subsequently, 10 μl of the amplified products was loaded on a 2% agarose gel and run for 1 h at 100 v. The gel was stained with ethidium bromide and photographed under UV light with the Gel printing 2000 system. The intensity of the bands was measured by densitometry using GPTools software. The amount of target gene amplified product was compared to that of the internal standard β-actin within the linear amplification range

using the following calculation, where intensity was the optical density of the band.

$$\text{Ratio of PCR product} = \frac{\text{intensity of target gene}}{\text{volume of target gene}} \times \frac{\text{volume of } \beta\text{-actin}}{\text{intensity of } \beta\text{-actin}} \quad (1)$$

Drug Treatment

Paclitaxel stock solutions were prepared in ethanol at 10 mg/ml and stored at –70°C. Aliquots of the stock solution was added to culture medium so that the final concentration of ethanol was <0.1%, which does not affect paclitaxel activity (18).

To evaluate whether the differences in the G2/M block and apoptotic effects of paclitaxel in MCF7 and BC19 cells resulted from the differences in intracellular drug accumulation, and to separate the efflux effect of Pgp from other biological consequences, we compared the drug effects in the two cell lines attained at equal extracellular and intracellular concentrations.

Measurement of Overall Drug Effect

Cells were seeded in 96 well microtiter plates (3,000–5,000 cells in 0.2 ml per well), and were allowed to attach to the plate surface by growing in drug-free medium for 20 to 24 h. Afterwards, cells were incubated with 0.2 ml of culture medium containing 0.1 to 10,000 nM paclitaxel for 96 h. There were six replicates for each concentration per plate. To avoid potential problems caused by evaporation of medium in wells located at the edge of the plate (which would alter the drug concentration), only the inner wells (rows 2 to 7 and columns 2 to 11) in the 96-well plates contained cells. The outer wells contained only the tissue culture medium, to serve as blanks.

The overall drug effect, which represents the combination of the antiproliferative and apoptotic effects of paclitaxel, was measured using the SRB assay. SRB stains for cellular proteins (19). In brief, after removing the drug-containing medium at the end of drug treatment, plates were rinsed 1 to 3 times with 0.2 ml phosphate-buffered saline (PBS) for about 10 min. The cells were then fixed by incubating with 0.05 to 0.2 ml of 10% trichloroacetic acid at 4°C for 1 h, followed by 5 washes with distilled water. SRB solution (0.035–0.15 ml, 0.4%) was added at room temperature for 10 min to stain the cells. Afterward, the plate was washed 5 times using 1% glacial acetic acid and allowed to air-dry overnight. Tris-HCl (10 mM, 0.2 ml per well) was then added to dissolve the SRB bound to cellular protein, which was measured by absorbance at 490 nm using an EL 340 microplate biokinetics reader (Bio-Tek™ Instruments Inc., Winooski, VT).

The relationship of paclitaxel-induced effect and drug concentration was analyzed by computer-fitting a sigmoidal pharmacodynamic function to the experimental data using nonlinear least square regression (NLIN; SAS, Cary, NC), as previously described (20). The pharmacodynamic function takes into account the residual unaffected cell fraction.

Measurement of Drug-Induced Apoptosis

Apoptosis was quantified by two methods. ELISA (Cell Death Detection ELISA kit, Boehringer Mannheim, Germany) was used to quantify the amount of DNA-histone complex released to the cytoplasm. In brief, 2.5×10^5 cells were plated in 25 ml flasks, allowed to attach to the flask for 20–24 h, and then treated with paclitaxel for 48 h. This treatment duration was selected because it resulted in readily detectable apoptosis. It is noted that we subsequently discovered that a 3 h treatment was sufficient to cause apoptosis, provided that apoptosis was measured after a lag time of 24 h (20). After treatment, attached cells were harvested by trypsinization and the detached cells dispersed in the culture medium were collected by centrifugation at 500 × g. Fifty thousand cells including both detached and attached cells were lyzed in lysis buffer, and the cytoplasmic fractions of the lysates were placed in a plate precoated with mouse anti-histone primary antibody and mouse anti-DNA antibody conjugated to peroxidase. The peroxidase substrate, 2,2′-azido-di-3-ethylbenzthiazoline sulfonate, was applied and the absorbance at 405 nm was measured.

The number of apoptotic cells after paclitaxel treatment was quantified using the ApoAlert Annexin V assay (Clontech Lab., Palo Alto, CA). Apoptotic cells lose membrane phospholipid asymmetry and expose phosphatidylserine on the outer leaflet of the plasma membrane (21). The externalized phosphatidyl-serine was labeled with Annexin V attached to a fluorescence probe FITC (green fluorescence). As apoptosis progresses, propidium iodide penetrates cell membrane and stains the cytoplasm (yellow-red stain). Briefly, cells were treated, harvested as described for the ELISA, suspended in 0.2 ml binding buffer, incubated with 10 μl Annexin V-FITC (0.5 μl/ml) and 10 μl propidium iodide (1 μl/ml) for 5–15 min in the dark, and examined by fluorescence microscopy using a dual filter at 488 nm. The numbers of labeled cells, including Annexin V-labeled cells that were in the early stage of apoptosis and cells that were doubly labeled with Annexin V and propidium iodide that were in the middle and late stages of apoptosis, were quantified.

Intracellular Accumulation of Paclitaxel

The procedures are as described previously (20). In brief, cells were plated at a density between $1.5–2.5 \times 10^4$ cells/ml in 25 ml flasks, and incubated with drug-free medium for 20–24 h. Afterward, the culture medium was replaced with 10 ml of medium containing mixtures of unlabeled paclitaxel and [^{3}H]paclitaxel (specific activity, 1.93–19.3 μCi/nmol). We previously showed in a drug uptake study that the intracellular and extracellular drug concentrations reached a pseudo steady state at ~4 h (22). Hence, the present study compared drug accumulation in MCF7 and BC19 cells after incubation for 8 h. After incubation, cells were washed twice with 5 ml of ice-cold versene and then harvested as a suspension after trypsinization. Cell number was determined using a Coulter Counter (Coulter Electronics Inc., Hialeah, FL), after dilution with 10–20 volumes of Isotone (Coulter Electronics, Inc.). To determine the radioactivity, samples were dissolved in 1 ml of Solvable Tissue Gel Solubilizer (Dupont, Boston, MA), mixed with 10 ml of Atomlight, and processed by liquid scintillation counting.

We have shown that over 95% of the intracellular radioactivity is represented by unchanged paclitaxel, and its bi-directional epimerization product 7-epitaxol. 7-Epitaxol accounts for <10% of total paclitaxel equivalence at 6 h, when

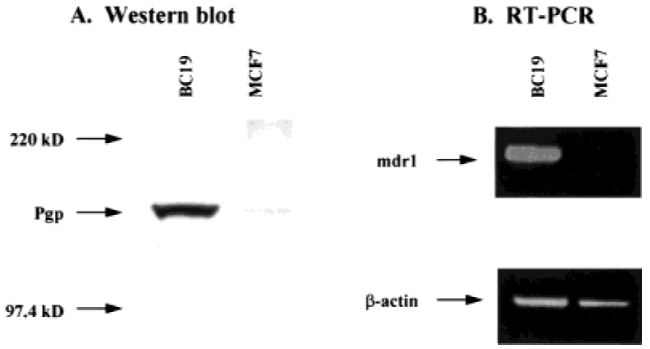

Fig. 1. Western blot analysis of Pgp level and RT-PCR analysis of *mdr*1 expression. (A) Western blot analysis of proteins. (B) RT-PCR analysis of expression of *mdr*1 mRNA.

the equilibrium between cells and medium has been reached (22). Compared to paclitaxel, 7-epitaxol has reduced polarity but identical microtubules binding affinity and cytotoxicity (23). Hence the total recovered radioactivity was taken as paclitaxel equivalents without further correction.

Intracellular drug concentration was expressed in molar term, by dividing the amount of drug per cell with the cell volume. A separate study used image analysis to determine the size of MCF7 and BC19 cells, and found no difference in their cell volumes, i.e. 2.09 and 1.96 μl per 10^6 cells, respectively (22).

Cell Cycle Analysis by Flow Cytometry

The distribution of cells in cell cycle phases was determined by standard flow cytometric analysis (24). In brief, 2.5 × 10^5 cells were plated in 25 ml flasks and allowed to attach to the flask for 20–24 h. Different concentrations of paclitaxel were then added. After 24 h treatment, cells attached to culture flasks were collected by trypsinization and the detached cells dispersed in the culture medium were collected by centrifugation at 500 × g. After washing with the washing buffer (1 mM EDTA, 1% bovine serum albumin or BSA in Hank's balanced salt solution) once, cells (attached plus detached) were dispersed into single cell suspensions which were fixed in ice-cold 70% ethanol for 30 min, and centrifuged at 1,000 × g for 2 min. After two washes in the washing buffer, cells were resuspended in 0.5 ml staining solution (40 μl/ml propidium iodide and 1 mg/ml RNase A in Hank's Balanced Salt Solution) and incubated at 37°C for 30 min. Samples were stored at 4°C for at least 1.5 h and analyzed by flow cytometry using a coulter EpicS Elite ESP cytometer (Coulter Corporation, Miami, FL). Single parameter DNA histograms from gated mode data were analyzed for cell cycle phase distribution using the multicycle AV (Phoenix Flow Systems, San Diego, CA). Modfit (Verity Software House, Topsham, ME) was used for cell cycle analysis.

Statistical Analysis

Differences in the results for the two cell lines were analyzed by the unpaired two-tailed Student's *t* test.

RESULTS

Pgp Level and *mdr*1 Expression

Figure 1A shows the Western blot analysis of Pgp level and Fig. 1B shows the results of the RT-PCR analysis of *mdr*1 expression. The level of Pgp in MCF7 cells was barely detectable whereas the level in BC19 cells was 9.3-fold higher. The RT-PCR results showed undetectable *mdr*1 expression in MCF7 cells and high *mdr*1 expression in BC19 cells. Compared to the level of *mdr*1 expression in a reference cell line, i.e. doxorubicin-resistant SKOV3 cells, where the expression was arbitrarily assigned a value of 100% (data not shown), the level of *mdr*1 expression was 133% in BC19 and <10% in MCF7. These results are in agreement with the literature data showing a much higher *mdr*1 expression in BC19 cells compared to MCF7 cells; the relative ratio of gene expression was 153% and <1% when compared to that in a reference cell line, i.e. doxorubicin-resistant AdrR MCF7 cells (16).

Accumulation of [^{3}H]Paclitaxel in Cells

Table I compares the intracellular accumulation of paclitaxel in MCF7 and BC19 cells, at various extracellular concentrations. At extracellular concentrations of ≤100 nM, drug accumulation in MCF7 cells was between 80% to 130% higher than in BC19 cells, which is in agreement with the higher Pgp level in BC19 cells. At higher extracellular concentrations of ≥1,000 nM, there were insignificant differences in drug accumulation (i.e., <15%), due to saturation of the Pgp-mediated efflux (25). Table I also shows that treatment of BC19 cells with 70, 350, 1,300, and 5,077 nM yielded approximately equal intracellular concentrations as in MCF7 cells treated with 10, 100, 1,000, and 5,000 nM. It is noted that the intracellular concentrations were 150- to 3,500-fold higher than the extracellular concentrations, due to the extensive binding of paclitaxel to intracellular components (4,20,22).

Table I. Intracellular Paclitaxel Accumulation in MCF7 and BC19 Cells

	Intracellular concentration, μM at the following extracellular concentrations								
Cell	1 nM	10 nM	70 nM	100 nM	350 nM	1,000 nM	1,300 nM	5,000 nM	5,077 nM
MCF7	2.0 ± 0.1	35 ± 1.2	NA	89 ± 5.2	NA	197 ± 18	NA	775 ± 53	NA
BC19	0.87 ± 0.16	13.8 ± 0.5	37 ± 0.8	50 ± 1.1	88 ± 4.7	175 ± 6.7	195 ± 9.3	671 ± 55	750 ± 45
p	<0.01	<0.01	NA	<0.01	NA	NS	NA	NS	NA

Note. Cells were incubated with various extracellular concentrations of [^{3}H]paclitaxel for 8 h, which was sufficient for intracellular drug concentrations to reach a steady state (22). The intracellular drug concentrations were determined and expressed in molar term. Note the different units for the intracellular and extracellular concentrations. Mean ± SD (n = 3). Statistical analysis of the differences was performed using the paired Student's *t* test. NA: not available. NS: not significantly different.

Overall Effects of Paclitaxel

Figure 2 shows the decrease in cell number by 96 h paclitaxel treatment, measured using the SRB assay. The extracellular drug concentration needed to produce a 50% reduction (IC_{50}) was 3.1 ± 0.7 nM (mean ± SD, $n = 3$) for MCF7 cells and 122 ± 34 nM for BC19 cells. The ratio of these IC_{50} values is 0.026.

Paclitaxel-Induced G2/M Block

Figure 3A shows the fraction of cells in the G2/M phase, as a function of extracellular drug concentrations. In the untreated controls, this fraction remained constant with time at 16%. In both MCF7 and BC19 cells, paclitaxel treatment produced a concentration-dependent increase in the cell fraction in the G2/M phase. MCF7 cells were more sensitive than BC19 cells to the G2/M block; the extracellular drug concentration needed to result in a 50% G2/M cell fraction was 9.1 ± 1.9 nM in MCF7 cells and 387 ± 93 nM in BC19 cells. The ratio of these concentrations is 0.023, which is comparable to the ratio of the IC_{50} values for the overall drug effect.

To determine whether the lower sensitivity of BC19 cells to the G2/M block effect of paclitaxel, compared to MCF7 cells, is due to the differential intracellular drug accumulation in the two cell lines and/or to other factors, we converted the extracellular concentrations displayed in Fig. 3A to their corresponding intracellular concentrations using the data in Table I. Figure 3B shows the G2/M block effect of paclitaxel as a function of the intracellular drug concentrations. The intracellular drug concentration needed to result in a 50% G2/M cell block was 29 ± 3 μM in MCF7 cells and 102 ± 14 μM in BC19 cells. These results demonstrate that the lower sensitivity of BC19 cells to the G2/M block effect of paclitaxel, compared to MCF7 cells, is partly due to the lower drug accumulation and partly due to the lower drug sensitivity in BC19 cells.

Paclitaxel-Induced Apoptosis

Figures 4A and 4B show the drug-induced apoptosis as a function of extracellular paclitaxel concentration, whereas Fig. 4C shows the apoptosis as a function of intracellular paclitaxel concentration. Because of the extensive paclitaxel accumulation in cells with an intracellular-to-extracellular concentration ratio of up to 1,000:1 (22), the intracellular concentrations such as those shown in Fig. 4C are much higher than the extracellular concentrations.

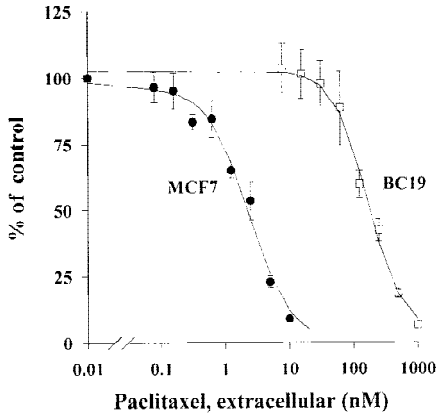

Fig. 2. Overall drug effect in MCF7 and BC19 cells induced by equal extracellular paclitaxel concentrations. MCF7 (●) and BC19 (○) cells. Lines are computer-fitted lines.

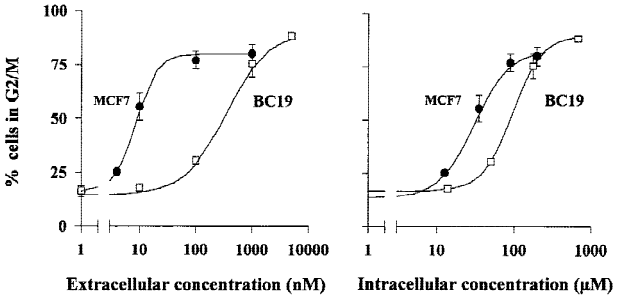

Fig. 3. G2/M block effect of paclitaxel in MCF7 and BC19 cells. (A) Data obtained at equal extracellular drug concentrations. (B) Data expressed as a function of intracellular concentrations corresponding to the extracellular concentrations displayed in Panel A. Symbols: mean ± SD of 2 to 4 experiments, duplicate samples for each experiment. Some SD are smaller than the symbols. Lines are computer-fitted lines. MCF7 (●) and BC19 (○) cells. Note the different units for extra- and intracellular concentrations.

Figure 4A shows the apoptotic indices as measured by the Annexin V-labeling technique and Fig. 4B shows the ELISA results of DNA-histone complex released into cytoplasm. In the absence of paclitaxel, both MCF7 and BC19 cells showed ~10% Annexin V-labeled cells, indicating no difference in the baseline apoptosis. Both measurements indicate qualitatively and quantitatively different concentration-apoptosis relationships in the two cell lines. In MCF7 cells, the apoptotic index and the level of cytoplasmic DNA-histone complex increased with paclitaxel concentration, but reached plateau values at 100 nM drug concentration with no significant increases even when the drug concentration was increased to 5,000 nM. In BC19 cells, these values continued to increase with drug concentration without reaching a plateau. The maximum apoptotic index in BC19 cells was twice that in MCF7 cells (i.e. 70% vs 35%). At equal extracellular

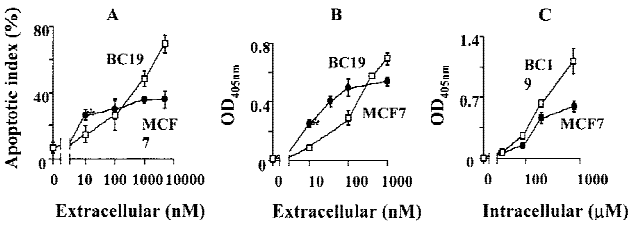

Fig. 4. Apoptotic effect of paclitaxel in MCF7 and BC19 cells. Top panels: Cells were treated with equal extracellular paclitaxel concentrations. The extent of drug-induced apoptosis in MCF7 (●) and BC19 (○) cells was measured by two methods. (A) The fraction of cells that externalized phosphatidylserine and stained with Annexin V was measured using the ApoAlert Annexin V assay. (B) The level of cytoplasmic DNA-histone complex was measured using ELISA. Bottom panel: MCF7 cells were treated with 10, 100, 1,000, and 5,000 nM extracellular paclitaxel concentrations, and BC19 cells with 70, 350, 1,300, and 5,077 nM. These extracellular concentrations yielded approximately equal intracellular paclitaxel concentrations (see Table I). Note the different units for extra- and intracellular concentrations. The level of cytoplasmic DNA-histone complex was measured using ELISA. Mean ± SD ($n = 3$). Some SD are smaller than the symbols.

concentrations, the apoptosis in MCF7 cells was initially higher at the lower concentration (e.g., 10 nM), but became equal or lower than the apoptosis in BC19 cells at higher concentrations (e.g., 100 nM for the apoptotic index measurement). A comparison of these data with the intracellular drug accumulation data in Table I suggests that the lower apoptosis in BC19 cells at extracellular drug concentrations of ≤100 nM was due to the 80 to 130% lower drug accumulation at these concentrations. Conversely, the higher apoptosis in BC19 cells at extracellular drug concentrations of ≥100 nM where the drug accumulation was comparable in BC19 and MCF7 cells suggests a higher sensitivity of BC19 cells to the apoptotic effect of paclitaxel. The latter was confirmed by the results in Fig. 4C, which shows the level of cytoplasmic DNA-histone complex as a function of intracellular drug concentration. In both MCF7 and BC19 cells, the drug-induced apoptosis became significantly elevated from the values of the untreated controls when intracellular drug concentrations were ≥89 μM. As the intracellular concentration increased, the apoptosis in MCF7 cells approached an asymptotic value whereas the apoptosis in BC19 cells continued to increase, similar to the observations in Figures 4A and 4B. The results in Fig. 4C further showed that the apoptosis in BC19 cells was consistently higher (between 30 to 100%) than that in MCF7 cells at all equal intracellular drug concentrations between 89 to 750 μM.

Collectively, the results in Figures 4A, 4B, 4C and Table I indicate that the concentration-dependent differences in the apoptosis of MCF7 and BC19 was partly due to the concentration-dependent intracellular drug accumulation in the two cell lines, and partly due to a higher sensitivity of BC19 cells to the apoptotic effect of paclitaxel.

DISCUSSION

The major findings of the present study are as follows. MCF7 cells are more sensitive than their *mdr*1-transfected variant BC19 cells to the G2/M block effect of paclitaxel, in part due to a higher intracellular drug accumulation in MCF7 cells and in part due to a greater sensitivity of the MCF7 cells. The pharmacodynamics of paclitaxel-induced apoptosis in MCF7 cells are qualitatively and quantitatively different from the pharmacodynamics in BC19 cells. The concentration-apoptosis relationship in MCF7 cells suggests a response that is nonlinear and becomes saturated at 100 nM extracellular drug concentration, whereas the relationship in BC19 cells suggests a response that is not saturated at extracellular drug concentration as high as 5,000 nM. The significantly higher apoptosis in BCl9 cells compared to MCF7 cells, at equal intracellular drug concentrations, indicate a positive correlation between Pgp expression and tumor cell sensitivity to apoptosis. Collectively, these findings confirm our observation in patient tumors that enhanced Pgp expression is associated with a greater sensitivity to the apoptotic effect by paclitaxel and a lower sensitivity to its G2/M block effect (15), and further indicate that these Pgp effects are exerted via mechanisms that are unrelated to the drug efflux effect of Pgp. It is noted that the higher apoptosis in the BC19 cells was attained at 100 nM extracellular drug concentration, which is a clinically achievable concentration (26).

Our finding of a higher sensitivity to paclitaxel-induced apoptosis in Pgp-expressing cells compared to Pgp-negative cells appears to disagree with the results of multiple studies which have shown an association between Pgp expression and resistance to several paclitaxel effects including reduction in cell number, reduction in colony-forming units, and apoptosis (27–32). This apparent disagreement can be explained by the different experimental models/conditions and the different effect endpoints used in our study and previous studies, as follows. First, the present study used cells that are stably transfected with *mdr*1 where Pgp expression is the only known difference, whereas some of the previous studies used cells where the resistance is induced by exposing cells to increasing concentrations of Pgp-inducing drugs (26–31). Resistant cells selected by this latter method may have other biologic changes, in addition to Pgp induction, that can affect their sensitivity to paclitaxel-induced apoptosis. For example, the paclitaxel-resistant HL-60/TAX 1000 cells contain 1.5- to 2.5-fold higher Bcl-2 level and 2.5 fold higher Bcl-X_L level compared to the parent HL-60 cells (29), and the paclitaxel-resistant J774.2 cells have altered expression of class II-β-tubulin isotype (30). Second, the present study specifically compared apoptosis whereas some of the previous studies compared the overall (e.g. reduction in cell number or colony forming units) or antiproliferative drug effects in Pgp-negative and Pgp-expressing cells (26–31). In general, the overall drug effect measured in exponentially growing monolayer cultures of human tumor cells, because of the high cell proliferation rate, is more reflective of the antiproliferative effect than of the apoptotic effect. Support for this argument is the similar concentration-response relationships between the overall drug effect and the G2/M block effect in MCF7 and BC19 cells (Figs. 2 and 3). In fact, if the overall drug effect data instead of the concentration-apoptosis relationship were used, one would arrive at the same conclusion as the previous studies, i.e., Pgp-expressing cells are more resistant than the Pgp-negative cells to paclitaxel. Specific and separate measurements of drug-induced G2/M block and apoptosis enabled the dissection of the differences in the pharmacodynamics of the two effects, and led us to conclude that Pgp-expressing cells are more sensitive to the apoptotic effect of paclitaxel. Third, the cell lines used in the various studies may be utilizing different apoptosis pathways. For example, the HL60 cells used in earlier studies were leukemia cells which are known to undergo primed apoptosis, where the present study used epithelial tumor cells which are known to undergo unprimed apoptosis (reviewed in 21). Fourth, as demonstrated in the present study, there is a complex relationship between extracellular drug concentration, intracellular drug accumulation, Pgp expression, and apoptosis. For example, at lower extracellular concentrations (i.e., ≤100 nM) where the Pgp-mediated drug efflux plays an important role in the drug efflux, the significantly lower intracellular drug concentrations in BC19 cells, as compared to MCF7 cells, resulted in an apparently lower apoptosis in BC19 cells. We observed a higher apoptosis in the BC19 cells only when the Pgp-mediated efflux becomes insignificant at higher extracellular concentrations (i.e., ≥100 nM) or when the differential drug accumulation is compensated by using comparable intracellular concentrations. Hence, the relationship between enhanced Pgp expression and increased sensitivity to apoptosis could only be detected/confirmed by experiments such as those in the present study specifically designed to address this issue.

In conclusion, *mdr*1 transfection resulted in a lower tumor cell sensitivity to the G2/M block effect of paclitaxel but a higher sensitivity to its apoptotic effect. These effects of *mdr*1 transfection were independent of the drug efflux mediated by p-glycoprotein. Studies to investigate the underlying mechanisms, including comparison of the expression and levels of apoptotic and anti-apoptotic genes and proteins, e.g., Bcl-2, Bax, and p53 (33), and comparison of drug distribution in subcellular organelles are ongoing in our laboratory.

ACKNOWLEDGMENTS

Supported in part by R37 CA49816 and R01 CA63363 from the National Cancer Institute, NIH, and a gift from the Bristol Myers Squibb Co. Dong Li was supported in part by the Pharmacia-Upjohn Fellowship. The Flow Cytometry Service of The Ohio State University Comprehensive Cancer Center was partly supported by the Cancer Center Support Grant P30CA16058 from the National Cancer Institute. The authors thank Seong Jang for his help with the drug uptake studies.

REFERENCES

1. E. K. Rowinski, M. Wright, B. Monsarrat, G. J. Lesser, and R. C. Donehower. Taxol: Pharmacology, metabolism and clinical implications. *Cancer Surveys* **17**:283–301 (1993).
2. P. B. Schiff and S. B. Horwitz. Taxol assembles tubulin in the absence of exogenous guanosine 5′-triphosphate or microtubule-associated proteins. *Biochemistry* **20**:3247–3252 (1981).
3. M. A. Jordan, K. Wendell, S. Gardiner, W. B. Derry, H. Copp, and L. Wilson. Mitotic block induced in HeLa cells by low concentrations of paclitaxel (taxol) results in abnormal mitotic exit and apoptotic cell death. *Cancer Res.* **56**:816–825 (1996).
4. M. A. Jordan, R. J. Toso, D. Thrower, and L. Wilson. Mechanism of mitotic block and inhibition of cell proliferation by taxol at low concentrations. *Proc. Natl. Acad. Sci. USA* **90**:9552–9556 (1993).
5. Y. Gan, M. G. Wientjes, D. E. Schuller, and J. L.-S. Au. Pharmacodynamics of taxol in human head and neck tumors. *Cancer Res.* **56**:2086–2093 (1996).
6. C. T. Chen, J. L.-S. Au, Y. Gan, and M. G. Wientjes. Differential time dependency of antiproliferative and apoptotic effects of taxol in human prostate tumors. *Urol. Oncol.* **3**:11–17 (1997).
7. J. L.-S. Au, J. Kalns, Y. Gan, and M. G. Wientjes. Pharmacologic effects of taxol in human bladder tumors. *Cancer Chemother. Pharmacol.* **41**:69–74 (1997).
8. N. J. Millenbaugh, Y. Gan, and J. L.-S. Au. Cytostatic and apoptotic effects of paclitaxel in human ovarian tumors. *Pharm. Res.* **13**:123–138 (1998).
9. Y. Gan, J. Lu, and J. L.-S. Au. Cytostatic and apoptotic effects of paclitaxel in human breast tumors. *Cancer Chemother. Pharmacol.* **42**:177–182 (1998).
10. S. B. Horwitz. Mechanism of action of taxol. *TIPS* **13**:134–136 (1992).
11. G. N. Hortobagyi and F. A. Holmes. Single-agent paclitaxel for the treatment of breast cancer: an overview. *Semin. Oncol.* **23**:4–9 (1996).
12. D. Nielsen, C. Maare, and T. Skovsgaard. Cellular resistance to anthracyclines. *Gen. Pharm.* **27**:251–255 (1996).
13. Y. Ito, M. Tanimoto, T. Kumazawa, M. Okumura, Y. Morishima, R. Ohno, and H. Saito. Increased P-glycoprotein expression and multidrug resistant gene (mdr1) amplification are infrequently found in fresh acute leukemia cells: Sequential analysis of 15 cases at initial presentation and relapsed stage. *Cancer* **63**:1534–1538 (1989).
14. J. E. Goasguen, J.-M. Dossot, O. Fardel, F. Le Mee, E. Le Gall, R. Lebla, P. Y. LePrise, J. Chaperon, and R. Fauchet. Expression of the multidrug resistance-associated p-glycoprotein (P-170) in 59 cases of de novo acute lymphoblastic leukemia: Prognostic implications. *Blood* **9**:2394–2398 (1993).
15. Y. Gan, M. G. Wientjes, and J. L.-S. Au. Relationship between paclitaxel activity and pathobiology of human solid tumors. *Clin. Cancer Res.* **4**:2949–2955 (1998).
16. C. R. Fairchild, J. S. Moscow, E. E. O'Brien, and K. H. Cowan. Multidrug resistance in cells transfected with human genes encoding a variant P-glycoprotein and glutathione-S-transferase π. *Molec. Pharmacol.* **37**:801–809 (1990).
17. T. Horikoshi, K. D. Danenberg, T. H. Stadlbauer, M. Volkenandt, L. C. C. Shea, K. Aigner, B. Gustavsson, L. Leichman, R. Frosing, M. Ray, N. W. Gibson, C. P. Spears, and P. V. Danenberg. Quantitation of thymidylate synthase, dihydrofolate reductase, and DT-diaphorase gene expression in human tumors using the polymerase chain reaction. *Cancer Res.* **52**:108–116 (1992).
18. L. R. Kelland and G. Abel. Comparative in vitro cytotoxicity of taxol and taxotere against cisplatin-sensitive and -resistant human ovarian carcinoma cell lines. *Cancer Chemother. Pharmacol.* **30**:444–450 (1992).
19. P. E. Pizao, D. M. Lyarun, G. P. Peters, J. van Ark-Otte, B. Winograd, G. Giaccone, and H. M. Pinedo. Growth, morphology and chemosensitivity studies on post-confluent cells cultured in 'V'-bottomed microtiter plates. *Br. J. Cancer* **66**:660–665 (1992).
20. J. L.-S. Au, D. Li, Y. Gan, X. Gao, A. Johnson, N. J. Millenbaugh, H. J. Kang-Kuh, J. Johnston, and M. G. Wientjes. Pharmacodynamics of immediate and delayed effects of paclitaxel: role of slow apoptosis and intracellular drug retention. *Cancer Res.* **58**:2141–2148 (1998).
21. J. L.-S. Au, N. Panchal, D. Li, and Y. Gan. Apoptosis: A new pharmacodynamic endpoint. *Pharm. Res.* **14**:1659–1671 (1997).
22. H. J. Kuh, S. H. Jang, M. G. Wientjes, and J. L.-S. Au. Computational model of intracellular pharmacokinetics of paclitaxel. *J. Pharmacol. Exp. Ther.* **293**:761–770 (2000).
23. I. Ringel and S. B. Horwitz. Taxol is converted to 7-epitaxol, a biologically active isomer, in cell culture medium. *J. Pharmacol. Exp. Ther.* **242**:692–698 (1987).
24. Z. Darzynkiewica, J. P. Robinson, and H. A. Crissman. *Methods in cell biology: Flow cytometry,* 2nd Edition, Part A, Academic Press, New York, 1995, pp. 32–36.
25. S. H. Jang, H.-J. Kuh, M. G. Wientjes, and J. L.-S. Au. Kinetics and mathematical modeling of paclitaxel efflux by p-glycoprotein in BC19 cells. *Proc. Am. Assoc. Cancer Res.* **39**:218 (1998).
26. D. S. Sonnichsen and M. V. Relling. Clinical pharmacokinetics of paclitaxel. *Clin. Pharmacokinet* **27**:256–269 (1994).
27. K. Bhalla, Y. Huang, C. Tang, S. Self, S. Ray, M. E. Mahoney, V. Ponnathpur, E. Tourkina, A. M. Ibrado, G. Bullock, and M. Willingham. Characterization of a human myeloid leukemia cell line highly resistant to taxol. *Leukemia* **8**:465–475 (1994).
28. S. B. Horwitz, L. Lothstein, J. J. Manfredi, W. Mellado, J. Parness, S. N. Roy, P. B. Schiff, L. Sorbara, and R. Zehab. Taxol: mechanisms of action and resistance. *Ann. NY Acad. Sci.* **466**:733–744 (1986).
29. J. Ark-Otte, G. Samelis, G. Rubio, S. J. B. Lopez, H. M. Pinedo, and G. Giaccone. Effects of tubulin-inhibiting agents in human lung and breast cancer cell lines with different multidrug resistance phenotypes. *Oncol. Rep.* **5**:249–55 (1998).
30. Z. Zhan, S. Scala, A. Monks, C. Hose, S. Bates, and T. R. Fojo. Resistance to paclitaxel mediated by P-glycoprotein can be modulated by changes in the schedule of administration. *Cancer Chemother. Pharmacol.* **40**:245–250 (1997).
31. Y. Huang, A. M. Ibrado, J. C. Reed, G. Bullock, S. Ray, C. Tang, and K. Bhalla. Co-expression of several molecular mechanisms of multidrug resistance and their significance for paclitaxel cytotoxicity in human AML HL-60 cells. *Leukemia* **11**:253–257 (1997).
32. M. Haber, C. A. Burkhart, D. L. Regl, J. Madafiglio, M. D. Norris, and S. B. Horwitz. Altered expression of Mβ2, the class II β-tubulin isotype, in a murine J774.2 cell line with a high level of taxol resistance. *J. Biol. Chem.* **270**:31269–31275 (1995).
33. D. Li, K. L. Koo, and J. L.-S. Au. P-glycoprotein overexpression increases maximum induction of apoptosis by taxol. *Proc. Am. Assoc. Cancer Res.* **39**:217 (1998).